LSST Science End-to-End Simulator: Implications for Weak Lensing

Simulator Purpose and Design:

We have developed a science end-to-end simulator for the full LSST system. The organization of the models for each component is based on a Monte Carlo history of each photon emitted by sky objects such as galaxies or stars. The input to the simulator is a model of the sky composed of galaxies and stars with their associated spectral energy distributions in the form of images with a fine spatial resolution much better than the LSST resolution. Multiple versions of the models can be simultaneously realized as a series of photons with precise sky locations and wavelengths. The final synthetic sky can be as simple as a grid of stars or as complex as a series of shells in z that comprise a 3D cosmological model composed of nearby stars, galaxies at intermediate z associated with dark matter and distant galaxies at high z that are distorted by the gravitational lensing of the emitted photons as they pass through dark matter at intermediate z. This versatility supports simulations of many types ranging from evaluation of PSF effects of the atmosphere on the images of stars and galaxies to the simulation and full analysis of a particular cosmological model. Also space-based images with fine angular resolution can be used directly as input sky models. The concept end-to-end refers to the history of the photons. The following list is the steps of the simulator:

- Photons are selected from a sky model using images and spectral energy distributions
- A set of atmosphere screens based on turbulence models are used to refract the photons
- Each photon is traced through the complete set of LSST optics
- Finally, the photons interact and are converted in a detector simulator and are readout

The wavelength dependence of the photons is modeled at all stages of the simulation process. The fidelity of the current version of the simulator is designed to include all details that affect science performance with an emphasis on weak lensing. Future versions will include details to support other science topics and secondary effects on weak lensing.

The atmosphere is modeled by a series of layers each with an independent 3D Kolmogorov model that is averaged into an equivalent screen with refractive index variations in 2D (Figure 1). Each layer has an outer scale, a random realization of gaussian amplitude phase independent Fourier modes with a seeing for each layer set by the Fried parameter R_0. The time dependence of the atmospheric seeing is modeled by the frozen translating screen approximation with a wind velocity and direction. The single photon history is traced through each layer of the atmosphere via a newly invented technique that avoids the need to do Fourier transforms of the wavefront perturbations. The approach is only valid for large aperture telescopes with exposure times of at least 10-20 seconds. A practical weak lensing simulation requires this approach since each photon from a faint galaxy (only 1000s) in a single integration (15 seconds) occurs at a different time within the exposure window for which the atmospheric structure has changed significantly. We can avoid Fourier transforms because the diffraction effects are averaged over a modest exposure (15 seconds) and over a large aperture (8 m). The figure below shows an example of a single Kolmogorov phase screen that spans a region of the atmosphere much larger than the aperture of the telescope. This allows for wind drifts during the exposure and for full wide field (3.5 degree diameter) images.

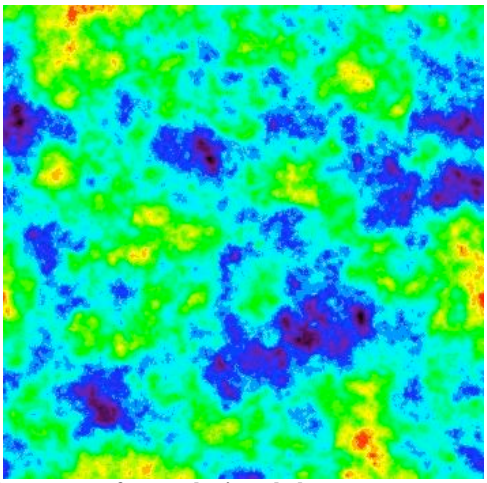

Fig 1: Phase screen of atmospheric turbulence

We have constructed a geometric raytrace code for the LSST designed optics. The raytrace handles reflection/refraction after calculating ray intercepts. The full wavelength-dependent refraction and filter transmission effects as well as stray light are included. Figure 2 shows the current LSST design and shows rays being reflected and refracted through the optics: the three mirrors, three lenses, the filter, and detector. On the surfaces of all the mirrors we currently apply a set of perturbations consisting of a set of orthogonal functions with a power spectrum resembling realistic perturbations found with the Kitt Peak 4m telescope when the active optics control system was operating. This model is designed to mimic the surface perturbations expected from thermal and mechanical distortions while a modern control system is being used.

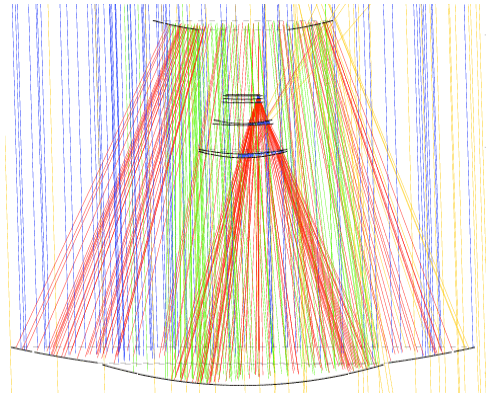

Fig 2: Raytrace of LSST optics

The current detector model built into the simulator treats conversion of individual photons into charge carriers collected at the channel. Each ray is refracted into the silicon according to its wavelength and incidence angle. The photon either interacts or doesn't interact, depending on its absorption range (dependent on wavelength and temperature of the silicon). The charge diffuses laterally during the time it takes to drift to the channel. The amount of diffusion is dictated by the strength of the electric field at the point of interaction.

The resulting PSF has limiting behavior in the two extremes of the instrument's band. The short wavelength achromaticity is broadened further by shallow interaction distribution in the CCD (contributing σ=4μm in each lateral dimension). On the long wavelength end, the PSF is dominated by the beam's refraction through the thick (100μm) silicon, combined with the large interaction length.

Figure 3 shows a simulation of the Hubble Ultra Deep Field simulated through the LSST end-to-end simulator. Every photon was raytraced using complete wavelength-dependent effects through 12 layers of atmospheric turbulence, the complete LSST designed optics, and the detector. Stars and galaxies were simulated from the UDF and sky noise background was added. Fields such as this are being used to practice analysis algorithms and evaluate the performance of the design of LSST for weak lensing systematics. The complete end-to-end simulation of a 800"x800" image (one CCD chip) takes only 20 hours on a single workstation due to extensive effort to make the code run as fast as possible. Approximately $3x10^8$ photons were simulated. Important simulation results are highlighted in the following section.

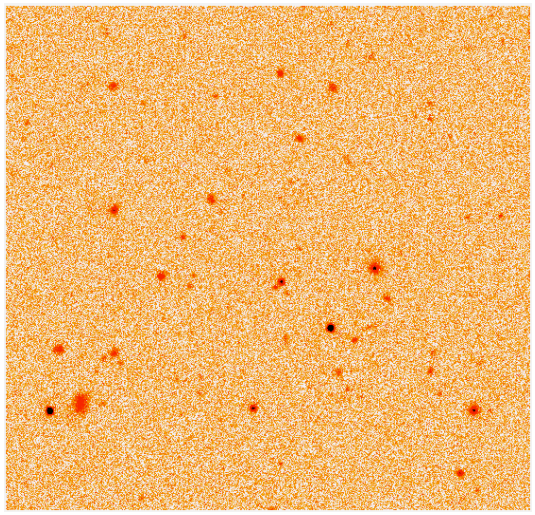

Fig 3: A small piece of a simulation of the Hubble UDF through the atmosphere and LSST optics and detector.

Implications for Weak Lensing Systematics:

The ellipticity of the point spread function (PSF) of any ground based telescope depends both on the properties of the atmosphere and the design and operation of the telescope and detector. Understanding the ellipticity of the PSF and its correlation across the field is critical to the success of weak lensing measurements. In particular, any residual uncorrectable ellipticity represents a floor that prevents the detailed measurements of arbitrarily low shear values.

Our simulations demonstrate that the ellipticity may receive similar contributions from

the optics and the atmosphere (1 to 2% for each), which is similar to the shear from a massive foreground cluster of galaxies. The optics contribution to the ellipticity of the PSF, however, is highly correlated on several hundred arcsecond scales. This is due to the fact that the secondary and tertiary mirrors in the LSST optics chain are relatively close to the pupil plane. Photons emitted from all points in the field of view see a similar part of the surfaces of all the mirrors. Every perturbation, therefore, affects the PSF across the field of view in a similar way. While it is important to control the overall ellipticity induced by the optics in the design of LSST, it is anticipated from these simulations that the optics contribution the ellipticity of the PSF will be easily correctable, since it is highly correlated. Studies are continuing to identify other instrumental problems that could affect weak lensing measurements.

Figure 4 demonstrates the expected PSF function when we turn on various parts of the simulator. The upper left image shows the PSF due to the optics alone with the mirror perturbations. The second image shows the PSF after the detector simulator is included. The lower left image shows the PSF when the atmosphere with no wind is included. The lower right shows the same but with wind. Clearly, the effect of wind reduces the ellipticity due to a larger part of the atmospheric turbulence that is being averaged.

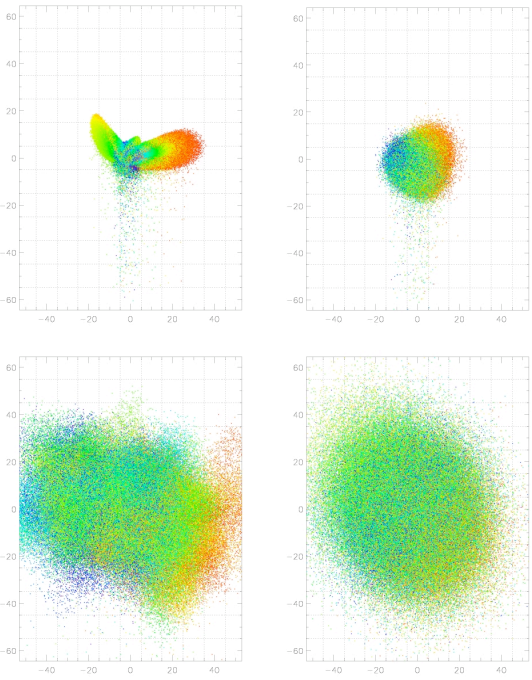

Fig 4: Simulated PSF of optics (upper left), optics+detector (upper right), atmosphere (lower left), atmosphere with wind (lower right). The colors represent where the photons hit the lsst aperture (red is the outer annulus, blue is the inner). The images are 120x100 microns, which is 2.4x2 arcseconds.

We have studied the effect of the atmosphere by generating grids of stars where the photons have been refracted by the atmospheric turbulence screens. Figure 5 shows the ellipticity vectors measured from a set of stars produced on an 18 arcsecond grid. One can see that the ellipticity is fairly well correlated from one point to the next even if this grid is only sparsely sampled by calibration stars. The simulations have shown that the decorrelation of the ellipticity as a function of angle depends on the overlap of projected telescope apertures at a given altitude such that the decorrelation angle is roughly equal to the telescope diameter over the layer height. Larger aperture telescopes will have a correlated ellipticity over larger angles.

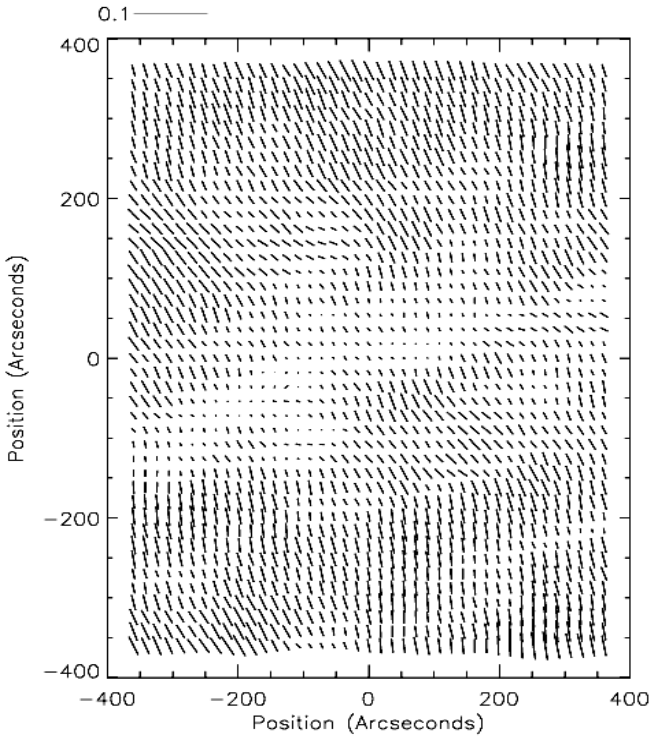

Fig 5: Ellipticity vectors of a grid of stars simulated through the atmosphere

Figure 6 shows a scatter diagram in which each dot represents a random pair of stars derived from grids of stars like those in Figure 5. Each pair has a separate angle and the magnitude ellipticity difference, $[(e_1\text{-}e')^2 + (e_2\text{-}e_2')^2]^{0.5}$, where each star has a vector ellipticity (e_1,e_2) and (e_1',e_2'). The weak lensing metric is defined as the

capability to accurately interpolate the PSF ellipticity at any arbitrary location in the field of view where a galaxy might be located based entirely on random calibration stars that are sufficiently bright. Figure 6 shows a comparison scatter diagram of data taken from a Gemini image (similar to LSST) and a simulated image with atmospheric effects included. This particular visualization emphasizes PSF difference effects on short angular scales (a few arc minutes) that are dominated by atmospheric effects. The telescope control system induces ellipticity effects in the PSF that vary over angles larger than 10 arcminutes. We are continuing a program to validate the atmospheric model with many different comparison tests with actual data. This particular visualization is just a sample to indicate the qualitative comparison of the PSF effects of the atmosphere both real and simulated.

Note the large variance of the ellipticity differences at every angular scale and the clear expected reduction in the average magnitude for angles approaching zero. The scatter diagram is different than the Gemini data near the origin due to higher shot noise in the real data. We have developed PSF interpolation procedures (not shown here) that fit the indicated ellipticity difference for angles less than 1 arc minute typical of the scale of separation of bright calibration stars at the Galactic poles. These interpolation methods reduce differences in ellipticities of $\sim 10^{-2}$ to $\sim 10^{-3}$ for single simulated image patches a few square arc minutes in size. The performance of the PSF interpolation schemes is similar for both simulated and real data. This performance means that Galaxy ellipticities can be corrected in single exposures at the $\sim 10^{-3}$ level.

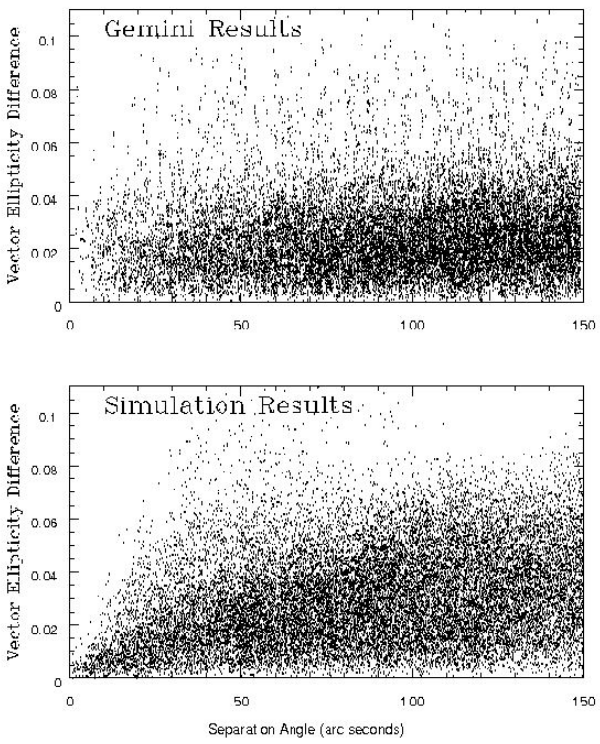

Fig 6: Vector ellipticity difference as a function of angle for simulations (bottom) and Gemini data (top). Gemini data was taken from a single 15 s exposure with the SLOAN r filter and the GMOS instrument. 243 stars were used in the 5.5x5.5' field of view.

The scatter diagram is useful for a visual comparison of PSF effects on short angular scales dominated by the atmosphere. The region near the origin for scales less than 1 arc minute indicates the correlation of the PSF that is required for the interpolation correction of the PSF for galaxies nearby calibration stars. We now consider a different metric that directly reveals the science performance for weak lensing measurement averaging over all atmospheric details. Figure 7 shows the shear correlation of a simulated atmosphere calculated in an identical way as described in the Subaru data appendix. The simulations demonstrate a similar decorrelation angle and lower shear residual. Further studies will validate the realism of the particular atmospheric model and the effect of the telescope on the residuals. The results are qualitatively similar.

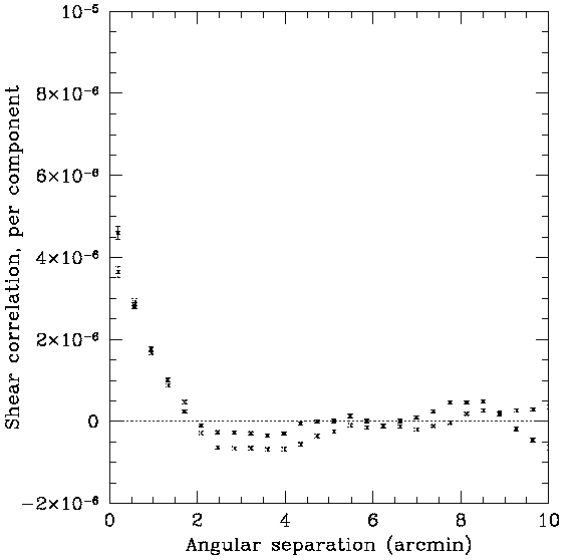

Fig 7: Shear correlation as a function of scale for the atmosphere simulations.